

Collective excitations of dipolar gases based on local tunneling in superlattices

Lushuai Cao,^{1,*} Simeon I. Mistakidis,² Xing Deng,¹ and Peter Schmelcher^{2,3,†}

¹*Ministry of Education Key Laboratory of Fundamental Physical Quantities Measurements, School of Physics, Huazhong University of Science and Technology, Wuhan 430074, People's Republic of China*

²*Zentrum für Optische Quantentechnologien, Universität Hamburg, Luruper Chaussee 149, 22761 Hamburg, Germany*

³*The Hamburg Centre for Ultrafast Imaging, Universität Hamburg, Luruper Chaussee 149, 22761 Hamburg, Germany*

(Dated: August 25, 2016)

The collective dynamics of a dipolar fermionic quantum gas confined in a one-dimensional double-well superlattice is explored. The fermionic gas resides in a paramagnetic-like ground state in the weak interaction regime, upon which a new type of collective dynamics is found when applying a local perturbation. This dynamics is composed of the local tunneling of fermions in separate supercells, and is a pure quantum effect, with no classical counterpart. Due to the presence of the dipolar interactions the local tunneling transports through the entire superlattice, giving rise to a collective dynamics. A well-defined momentum-energy dispersion relation is identified in the ab-initio simulations demonstrating the phonon-like behavior. The phonon-like characteristic is also confirmed by an analytical description of the dynamics within a semiclassical picture.

I. INTRODUCTION

Collective excitations constitute a fundamental concept in condensed matter physics which is at the origin of various phenomena in the field [1, 2]. Remarkable examples of collective excitations are phonons, magnons or plasmons. Among them, phonons describe the collective dynamics of the atomic vibrations in the crystal lattice, and play a key role for different fundamental effects in condensed matter physics, such as superconductivity [3] or the thermal transport in solid matter [4, 5].

Generalizations of the concept of a phonon can be found in ion traps [6, 7] or ultracold dipolar quantum gases [8, 9]. Phonons in ion traps refer to the collective dynamics of ions' motion around their equilibrium positions in e.g. Paul traps. In dipolar quantum gases, it describes the coupling between the local vibrations of dipolar atoms in a self-assembled chain or a lattice. Generally speaking, phonons in crystals, ion chains and dipolar lattices all refer to the collective dynamics of vibrations, which have a direct analogue to the motion of classical vibrators, and these phonons can be seen as a direct extension of the classical dynamics of a vibrating chain to the quantum regime. Here, we introduce a new type of collective dynamics in ultracold dipolar gases in a one-dimensional superlattice. The key ingredient for this collective dynamics is a local tunneling, which possesses no classical counterpart.

Our investigation is mainly based on ab-initio simulations, besides a semiclassical analytical treatment. The simulations are performed by employing the numerically exact Multi-Layer Multi-Configuration Time-Dependent Hartree method for identical particles and

mixtures (ML-MCTDHX) [10], which has been developed from MCTDH [11, 12], ML-MCTDH [13, 14] and ML-MCTDHB [15, 16], and has a close relation to MCTDHB(F) [17–19]. The ab-initio simulations of the corresponding ultracold quantum gases take into account all correlations, and can unravel new effects beyond the predictions of mean-field theory and for lattice systems beyond the single-band Bose-Hubbard model. Representative examples along this line are the loss of coherence and the decay of contrast of different types of solitons [20, 21], higher band effects on the stationary [22] or dynamical properties [23–28] in optical lattices. To investigate the collective dynamics in the double-well superlattice, we employ ML-MCTDHX which allows for a full description of the dynamics, and proves the robustness of the collective dynamics against higher order correlations and higher band effects.

This work is organized as follows: In section II, we present an introduction to the detailed setup (Sec. II.A), the initial state preparation (Sec. II.B), the local effect of the perturbation that drives the system out of equilibrium (Sec. II.C), and the global collective dynamics induced by the local perturbation (Sec. II.D). We also supply a semiclassical analytical description of the collective dynamics (Sec. II.E). The discussion of our results and the conclusions are provided in section III.

II. COLLECTIVE EXCITATIONS BASED ON LOCAL CORRELATION-INDUCED TUNNELING

A. Setup

We consider a dipolar superlattice quantum gas (DSG) composed of N spin-polarized fermions confined in a one-dimensional double-well superlattice of N supercells, *i.e.* a unit filling per supercell. All the fermions interact with

* lushuai.cao@hust.edu.cn

† pschmelc@physnet.uni-hamburg.de

each other by dipolar interactions. The Hamiltonian read as follows

$$H = \sum_{i=1}^N \left(\frac{-\hbar^2}{2M} \partial_{x_i}^2 + V_{sl}(x_i) \right) + \sum_{i < j=1}^N \frac{D}{|x_i - x_j|^3 + \delta}. \quad (1)$$

The first term refers to the single-particle Hamiltonian, where V_{sl} models the double-well superlattice with $V_{sl}(x) = V_0(\sin^2(kx) + 2\cos^2(2kx))$. This superlattice can be formed by two pairs of counter-propagating laser beams of wave vectors k and $2k$, and the strength of the lattice V_0 can be tuned by the amplitude of the laser beams. We consider a finite-length lattice of N supercells, and hard-wall boundaries are applied at positions $x = \pm N\pi/(2k)$, to allow only N supercells in our simulation. The second term in the Hamiltonian models the dipolar interaction between the fermions. In this work we consider the situation that all the dipoles are polarized along the same direction, perpendicular to the relative distance between the fermions, and D denotes the strength of the interaction. To avoid in simulations the divergence of the interaction at $x_i = x_j$, an offset δ is added to the denominator. The offset δ takes a rather small value, which is about eight times smaller than the spacing of the discrete grid points chosen within our simulations. More specifically, in the present work we focus on the situation where all fermions reside in different wells for which case the distances where a significant overlap exists are much larger than δ . Then, the offset is negligible.

In order to investigate the collective excitations, the DSG is firstly relaxed to the ground state of H , and at $t = 0$ a local perturbation is applied to a single supercell of the lattice, *e.g.* the outer most left cell is taken out of equilibrium. This perturbation is intended to induce a local dynamics in the left cell, and is applied only for a short time period, to avoid affecting the global dynamics on a long time scale. We model the local and temporal perturbation by $V_{pt}(x, t) = V_1 \theta(x + (N - 1)\pi/(2k)) \theta(t - \tau)$, with the Heaviside step function $\theta(x)$. The perturbation is then modeled as a local step function applied to the outer most left supercell and lasts only for the temporal interval $[0, \tau]$. The double-well superlattice and the local perturbation are sketched in figure 1 for five fermions in a five-cell superlattice. In the simulation, we render the Hamiltonian dimensionless by setting $\hbar = M = k = 1$, which is equivalent to rescaling the energy, space and time in the units of $E_R = \hbar^2 k^2 / 2M$, k^{-1} and \hbar / E_R , respectively.

The setup discussed above can be realized in ultracold atom experiments. Moreover, dipolar quantum gases have become a hot topic in the field of ultracold atoms and molecules [29, 30]. Their rich phase properties [31–35] and perspectives in, for instance, quantum simulations [36–38] have inspired extensive studies on dipolar quantum gases. Experiments can nowadays prepare dipolarly interacting particles in lattices, due to the rapid development of cooling atoms [39–41] with large magnetic

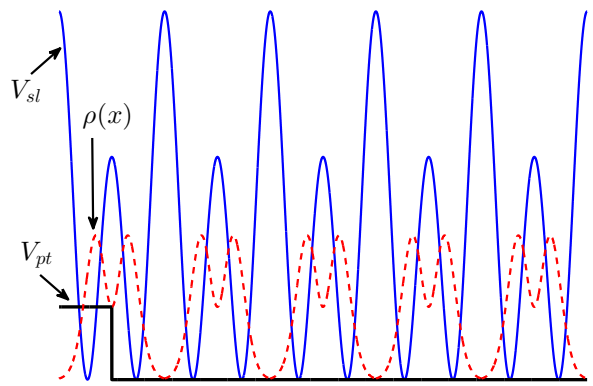


FIG. 1. Sketch of the dipolar fermionic gas in a double-well superlattice of five cells. The blue and black lines show the double-well superlattice and the local perturbation modeled as a step function applied only to the most left site of the lattice, respectively. Five fermions (red dashed gaussians) are loaded to the superlattice, each of which is localized in a different supercell and occupies the two sites in the cell for the initial state.

dipole moments and polar molecules in optical lattices [42–46]. Specifically, the double-well superlattice has been realized in experiments, and has become a widely used testbed for various phenomena, such as correlated atomic tunneling [47], generation of entanglement of ultracold atoms [48] and the topological Thouless quantum pump [49]. The setup discussed and analyzed here is therefore well within experimental reach.

B. Paramagnetic-like initial state

The dynamics investigated in the present work strongly depends on the choice of the initial state, which is prepared as the ground state of H in a particular parameter regime. It has been shown [50] that the DSG system can be mapped to an effective Ising spin chain model under the so-called pseudo-spin mapping. Then, within the Ising spin picture the ground state of the system undergoes a transition from a paramagnetic-like state to a single-kink state for increasing dipolar interaction. The paramagnetic-like state refers to the pseudo-spins polarized in the same direction due to an effective magnetic field, whereas the single-kink state is composed of two effective ferromagnetic domains aligning in opposite directions. In the present work, we focus on the dynamics in the weak interaction regime, *i.e.* the DSG system initially resides in the paramagnetic-like state.

To comprehend and analyze qualitatively the initial particle configuration (being characterized by the many-body state $|\Psi\rangle$) we shall employ the notion of reduced densities. The one-body reduced density matrix $\rho_1(x, x') = \langle x' | \hat{\rho}_1 | x \rangle$, is obtained by tracing out

all fermions but one in the one-body density operator $\hat{\rho}_1 \equiv \text{tr}_{2,\dots,N} |\Psi\rangle\langle\Psi|$ of the N -body system, while the two body density $\rho_2(x_1, x_2) = \langle x_1, x_2 | \hat{\rho}_2 | x_1, x_2 \rangle$ can be obtained by a partial trace over all but two fermions of the two-body density operator $\hat{\rho}_2 \equiv \text{tr}_{3,\dots,N} |\Psi\rangle\langle\Psi|$. Subsequently, the initial state can be characterized by the two-body and one-body correlations in the superlattice, as shown in figure 2. Figure 2(a) presents the two-body correlation of five fermions in a five-cell superlattice. The vanishing occupation along the diagonal direction in the two-body correlation illustrates that no two fermions (or more) occupy the same supercell, and each supercell hosts only one fermion, which is a Mott-like configuration. Being localized in a separate supercell, the fermions can occupy the left and right sites of the cell simultaneously, giving rise to particle number fluctuations in these sites and in particular to a non-vanishing off-diagonal one-body correlation, as shown in figure 2(b). This non-vanishing one-body correlation plays a key role in the collective dynamics investigated in the present work.

To a good approximation, the paramagnetic-like ground state (see also Appendix B) can be expressed as

$$|G\rangle = \sqrt{2^{-N}} \prod_{i=1}^N (|L\rangle_i + |R\rangle_i), \quad (2)$$

where $|L\rangle_i$ and $|R\rangle_i$ denote the lowest-band Wannier states in the left and right site of the i -th supercell, respectively.

C. Correlation-induced tunneling in a single supercell

To drive the system out of equilibrium from the initial state $|G\rangle$, we apply a local perturbation V_{pt} to the most left supercell. The perturbation is intended to induce a local tunneling of the fermion in this supercell and is modeled by a step function applied to the left site of the supercell. In this subsection we describe the local dynamics in this supercell under the perturbation V_{pt} . The step function introduces an energy offset between the left and right sites of the cell. Normally, the energy offset inhibits the tunneling between the two sites, of which the amplitude is reduced, by increasing the amplitude of the offset. When a particle is initially prepared in a superposition state involving the two sites equally, however, the offset can enhance the tunneling of the particle in a narrow parameter window of the offset strength. The tunneling amplitude becomes maximal when the strength of the perturbation matches that of the hopping between the two sites.

The explanation of such an unusual tunneling is as follows: In the normal case, the energy offset breaks the resonance between the two sites in terms of the potential energy, and thus it inhibits the tunneling between

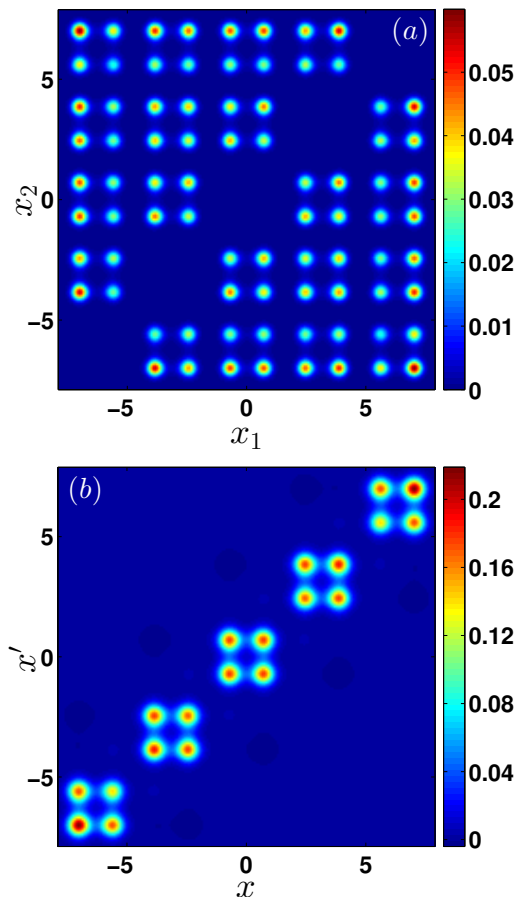


FIG. 2. (a) The two-body correlations and (b) one-body correlations of the initial state of five fermions in a five-cell superlattice. The two-body correlation illustrates that any two fermions cannot occupy the same supercell, *i.e.* each supercell hosts a single fermion. The off-diagonal of the one-body correlations indicates the delocalization of the fermion between the left and right sites of the supercell. The parameters used here are $(V_0, D) = (10, 0.3)$, which correspond to a weakly interacting dipolar gas in a deep superlattice.

the two sites. When the initial state is chosen as a superposition state of the particle occupying the two sites equally, a finite kinetic energy is stored in the system. The finite kinetic energy can then compensate the resonance breaking of the potential energy and promote the tunneling. The maximum compensation is reached when the energy offset matches the initial kinetic energy, which can be realized when the strength of the offset equals the hopping strength. In the double well system, the kinetic energy coincides with the one-body correlation between the two sites, up to a factor determined by the hopping strength, and we term this unusual tunneling as correlation induced tunneling (CIT) [51], to indicate the connection between the kinetic energy and the one-body spatial correlation. Moreover, the CIT can also be viewed as a Rabi oscillation between the two states $(|L\rangle \pm |R\rangle)/\sqrt{2}$, where the tilt couples these two states and determines

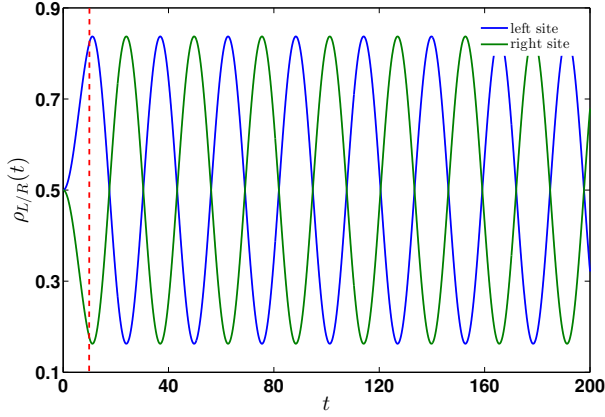


FIG. 3. Density oscillation of a single particle in a double well with a local perturbation applied to the left well. The local perturbation is applied for a short time period, and the red dashed line marks the time when it is turned off. The double well is taken from a single unit cell of the superlattice with $V_0 = 10$, and the height of the perturbation potential is $h_1 = 0.1$.

the corresponding Rabi frequency. In figure 3 we illustrate the CIT of a single particle confined in a double well potential with a temporal energy offset. To proceed we calculate the population of each well, e.g. for the right well $\rho_R(t) = \int_0^\pi dx \rho_1(x, t)$ (with ρ_1 being the one-body density). As shown in the figure, initially the particle is occupying both sites with equal probability, and after the perturbation (applied at $t = 0$), the probability oscillates from the right to the left well, indicating a tunneling between the two wells. When the perturbation is turned off (the turn-off time is marked by the dashed red line in figure 3), we observe that the tunneling persists. Turning to the whole superlattice, it can be expected that the CIT also takes place in the left supercell when the same perturbation is applied to a double-well supercell.

D. Collective dynamics of local CIT

Having introduced the initial state and the local dynamics of the CIT, let us proceed to the global dynamics of the entire DSG system being subjected to a local perturbation. Our main finding can be summarized as follows: Once the local perturbation induces the CIT in a single supercell, e.g. the most left one as considered here, the dipolar interaction can transport the local CIT to other cells. In this manner, all the fermions, while remaining well localized in their separate supercells, perform local CIT between the two sites of their supercells, giving rise to a collective dynamics of local CIT in the DSG system. Moreover, the collective dynamics resembles phonon-like excitations, with a well defined momentum-energy dispersion relation. In following, we shall demonstrate the collective dynamics of local CIT

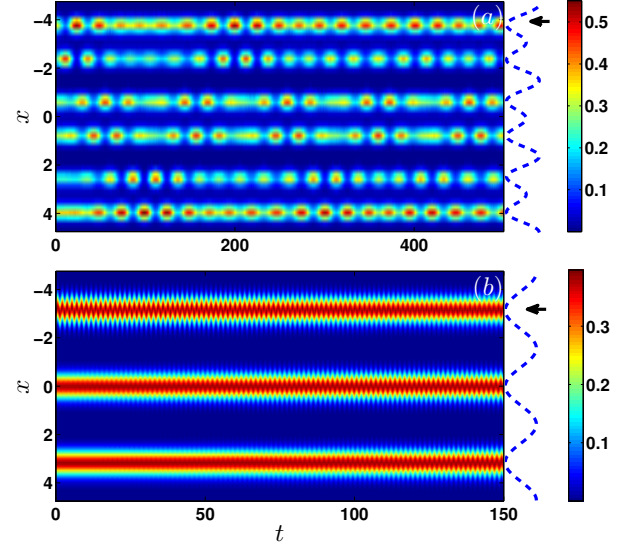


FIG. 4. (a) The density evolution $\rho_1(x, t)$ of a three-fermion system in a three-cell superlattice, and (b) in a plain triple well, under a corresponding local perturbation. The dashed lines attached to the right of the figures illustrate the corresponding trapping potentials. The arrows mark the position where the local perturbation is applied for both cases. The parameters used here and in figure 5 are $(V_0, D, V_1) = (10, 0.3, 0.1)$.

employing ab-initio simulations.

Firstly, we simulate the collective dynamics of $N = 3$ fermions confined in a three-cell superlattice, i.e. a 3F3C (3 fermions in 3 cells) system, and compare it with the phonon of three dipolar-interacting fermions in a plain triple well. In figure 4(a) we show the one-body density oscillation $\rho_1(x, t)$ of the 3F3C system under the perturbation V_{pt} . We observe that CIT takes place in all the three supercells, with no inter-cell tunneling between neighboring supercells. This collective dynamics of CITs is different from the dipolar phonon as well as the ion phonon, which refer to the collective dynamics of local classical vibrations of dipolar atoms or ions confined in a lattice respectively. In figure 4(b) we also present the one-body density of the dipolar phonon of three fermions in a plain triple well. In the dipolar phonon case, a local tilt induces a dipole oscillation of the fermion in the left well, and the dipolar interaction transports the local density oscillation to fermions in remote wells, giving rise to the collective phonon dynamics. Firstly, a similarity can be drawn between the collective CIT and the dipolar phonon, where both cases are composed of local dynamics coupled by the dipolar interaction. On the other hand, the distinction of the two collective dynamics is also obvious: The dipolar phonon (as well as the ion phonon) is composed of local oscillations of particles and can be seen as a direct extension of the classical phonons to the quantum regime. Meanwhile, the collective dynamics of CIT has no counterpart in the classical world and is a

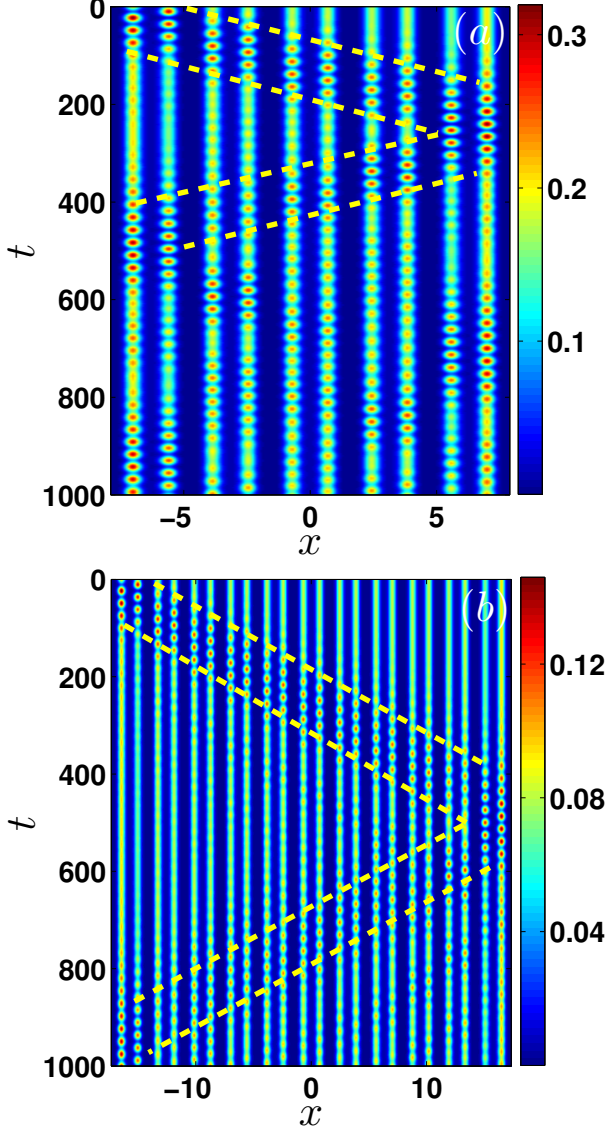


FIG. 5. The density evolution $\rho_1(x, t)$ of (a) a five-fermion and (b) eleven-fermion system of unit-filling, under the local perturbation. The dashed yellow lines in both figures illustrate the finite transport velocity of the local CIT through the superlattice. The dashed lines (see the corresponding slopes) also suggest an equal transport velocity of the CIT in both systems, implying that the transport velocity is independent of the system size.

pure quantum effect.

To demonstrate the generality of such collective dynamics with respect to the size of the superlattice we show that the same behavior is evident in 5F5C (5 fermions in 5 cells) and 11F11C (11 fermions in 11 cells) systems, as shown in figures 5(a) and 5(b), respectively. In both figures we observe that the collective dynamics of local CIT indeed takes place in bigger systems, indicating that it is not restricted to a particular size. Moreover, in the longer lattices, we observe more clearly how the

local CIT transport through the whole system: They are not simultaneously excited along the lattice once the perturbation is applied, but the CIT are transported with a finite velocity from the left supercell to remote ones. The transport of local CIT with a finite velocity is illustrated in both figures with the yellow dashed lines, where one can even observe the reflection at the edges of the lattice. In this way, the collective dynamics of local CIT in the DSG systems also serve as a test bed for the light-cone like behavior of two-body correlations.

It is known that all phonon-like collective excitations share a common property of well defined momentum-energy dispersion relation, where the collective dynamics can be decomposed into a set of momentum modes and each mode has a well defined energy, *i.e.* characteristic frequency. It is interesting to investigate whether the collective dynamics of DSG systems is also associated with a dispersion relation. For this purpose, we calculate the density difference between the left and right sites of each supercell $\delta\rho(i, t)$ ($i \in [1, N]$), and further define a set of k -modes as

$$\delta\tilde{\rho}(k, t) = \sum_{n=1}^N \sin\left(\frac{nk\pi}{N+1}\right) \delta\rho(n, t), k \in [1, N] \quad (3)$$

To verify the corresponding dispersion relation we then calculate the spectra of $\delta\rho(i, t)$ and $\delta\tilde{\rho}(k, t)$. We show the spectra of $\delta\rho(1, t)$ for 5F5C and 11F11C in figures 6(a₁) and 6(b₁), respectively, and the corresponding spectra of $\delta\tilde{\rho}(k, t)$ in figures 6(a₂) and 6(b₂). These figures demonstrate that, firstly the spectra of $\delta\rho(i, t)$ show N main peaks for the N -fermion system, each of which corresponds to one k -mode, indicating that the collective dynamics can be indeed decomposed into N k -modes. More importantly, each k -mode is associated with a dominant frequency peak, as shown in the spectra of $\delta\tilde{\rho}(k, t)$, and this directly verifies a well-defined momentum-energy dispersion relation in the collective dynamics of the CIT. Further, we also observe some weakly pronounced peaks lying near zero in the spectra, which are close to the values of the frequency difference between the corresponding peaks. These peaks are attributed to a weak nonlinear effect similar to phonon-phonon interactions.

E. Semiclassical description of the collective CIT dynamics

In this section, we supply a semiclassical description of the collective CIT excitation, in terms of $\langle\delta\rho(i, t)\rangle$. The starting point is the second-order time derivative equation

$$-\partial_t^2 \langle\delta\hat{\rho}(i, t)\rangle = \langle[[\delta\hat{\rho}(i), \hat{H}], \hat{H}]\rangle, \quad (4)$$

which is derived simply by applying $i\partial_t \langle\delta\hat{\rho}(i, t)\rangle = \langle[\delta\hat{\rho}(i), \hat{H}]\rangle$ twice, while the notation $\langle...\rangle$ denotes the expectation value $\langle\Psi(t)|...|\Psi(t)\rangle$. Then the major task of solving equation (4) is to find proper expressions of the

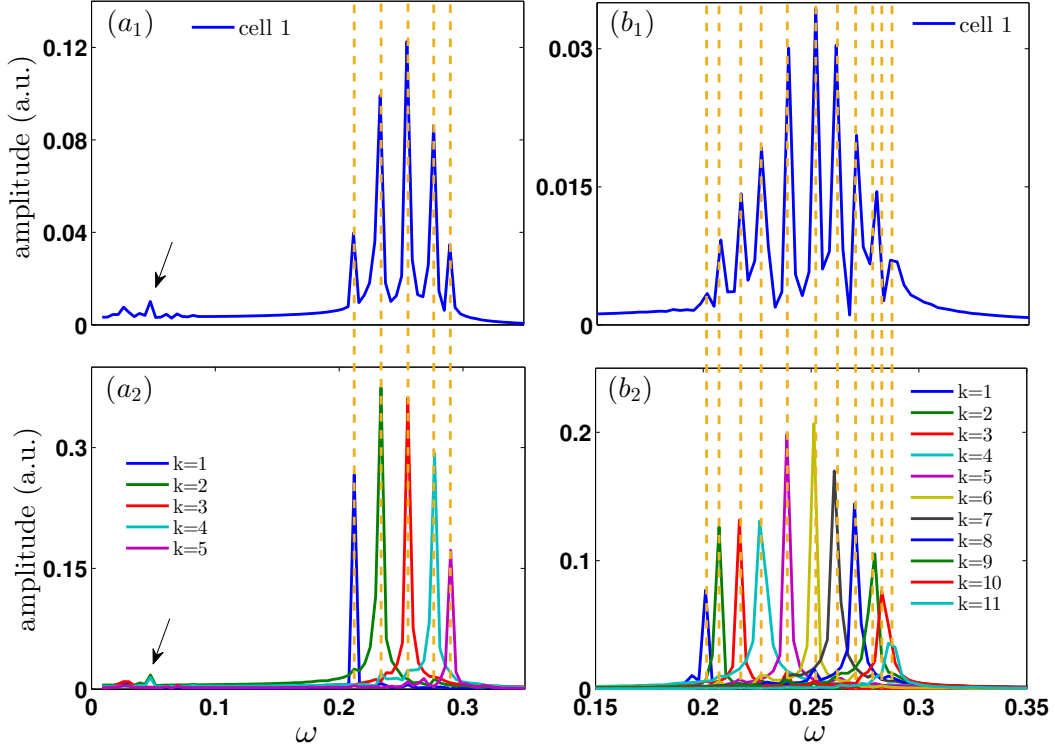


FIG. 6. The frequency spectra for a five-fermion (left column) and eleven-fermion (right column) system of unit-filling. The upper and bottom rows correspond to the spectra of $\delta\rho(1, t)$ and the k modes $\delta\tilde{\rho}(k, \omega)$, respectively. The dashed vertical lines demonstrate a one-to-one correspondence between the peaks in $\delta\rho(1, t)$ to the peak of a particular k -mode peak. The arrows in figures (a_1) and (a_2) mark the tiny peaks in the low-frequency regimes, which are understood as a nonlinear effect of frequency subtraction. As a result of the low resolution of the spectra with respect to the dense packing of the peaks in the 11F11C case, some peaks are not well presented in figure (b_1) .

Hamiltonian \hat{H} (for more details see Appendix B and in particular equation (B1)) and to solve for $|\Psi(t)\rangle$.

We adopt the lowest-band Hubbard model for \hat{H} and apply degenerate perturbation theory to solve for $|\Psi(t)\rangle$ and derive a set of closed equations for $\langle\delta\hat{\rho}(i, t)\rangle$: a detailed derivation is given in Appendix B. The final form of the equations that $\langle\delta\hat{\rho}(i, t)\rangle$ obeys, reads

$$-\partial_t^2 \langle\delta\hat{\rho}(i, t)\rangle = 4J^2 \langle\delta\hat{\rho}(i, t)\rangle + 4JV (\langle\delta\hat{\rho}(i-1, t)\rangle + \langle\delta\hat{\rho}(i+1, t)\rangle), \quad (5)$$

where J and V refer to the intra-cell hopping and the dipolar interaction strength, respectively. Equation (5) is the semiclassical version of equation (4), and it is clear that equation (5) resembles that of classical vibrating chains, where $\langle\delta\hat{\rho}(i, t)\rangle$ plays the role of the local displacement of the i -th vibrator. The general solutions of equation (5) correspond to a set of eigenmodes, and a particular solution is given by the superposition of these eigenmodes (equation corrected)

$$\langle\delta\rho(i, t)\rangle = \sum_{k=1}^N (C_k \sin(\omega_k t) + D_k \cos(\omega_k t)) \sin\left(\frac{ki\pi}{N+1}\right), \quad (6)$$

where $\omega_k = \sqrt{4J[J + 2V \cos(k\pi/(N+1))]}$, and C_k, D_k are determined by the initial state. The semiclassical equations (5) and their eigenmode solutions (see equation (6)) directly illustrate the phonon-like behavior of the collective dynamics of the local CIT in the DSG system.

III. DISCUSSION AND CONCLUSIONS

In this work we demonstrate a new type of collective excitations in dipolar quantum gases confined in the double-well superlattice with a unit filling factor. The collective excitations manifest themselves as the coupling and transport of local CIT within each supercell. The local CIT are a pure quantum effect and have no classical counterpart, which endows the dynamics composed of these collective excitations with a pure quantum nature, instead of being a quantum correction to any classical dynamics.

These collective excitations can also be generalized from the double-well superlattice to more complicate superlattices, where new properties of the collective dynamics can be engineered. For instance, the CIT in a double well possesses a single characteristic frequency,

and in the spectrum of the collective dynamics a single band arises from this characteristic frequency. When the supercell is expanded to multiple wells, the corresponding characteristic frequencies of the local CIT will also increase, and each of these frequencies seeds a band in the spectrum of the collective dynamics of the local CIT, resulting in a multi-band spectrum. The tunability of the band structure by the supercell properties indicate a high flexibility in designing and engineering new properties of such collective excitations. Meanwhile, in the relatively strong interaction regime, one can expect more pronounced nonlinear effects, such as the scattering of the collective excitations, which, however, is beyond the scope of the current work.

It is in place to discuss the realizability and robustness of the collective excitations under realistic conditions. Firstly, these excitations are not restricted to fermionic dipolar gases, but can also be realized with bosonic dipolar gases, as the particles are localized in separate cells and the particle statistics plays almost no role here. For realistic implementations, the collective excitations may be blurred by effects due to finite temperature, an additional external potential and the imperfectness of the filling factor. To observe collective excitations, it is required to cool the particles to the lowest band of the lattice. In previous experiments on double well superlattices, this condition has been fulfilled for contact interacting atoms, and with the fast progress in cooling dipolar lattice gases we expect this condition will become also feasible for our setup. In experiments, the confinement of lattice gases to a finite spatial domain is realized by an external harmonic trap, which will also introduce some constraints on the realization. In the bottom of the harmonic trap, it is possible to prepare a paramagnetic-like state, while at the edge deviations from the perfect paramagnetic-like configuration can arise. It has been shown that this edge effect will not change the global paramagnetic-like configuration [50], and we also note that it is now possible to compensate the extra harmonic trap with a dipole trap in experiments [52], which can further release the constraints. Finally if the filling deviates from unit filling per supercell, holes or doublons can arise in the superlattice, which can scatter and couple to the collective excitations. New phenomena can be generated due to such scattering and coupling, and we refer the reader for possible new phenomena to future investigations.

ACKNOWLEDGMENTS

This work is dedicated to Prof. Lorenz Cederbaum on the occasion of his 70th birthday. The authors acknowledge the efforts of Sven Schmidt and Xiangguo Yin in the initial stage of the work. L. Cao is also grateful to Antonio Negretti for inspiring discussions on ion phonons and the conditions of realistic implementations. S.M and P.S gratefully acknowledge funding by the Deutsche Forschungsgemeinschaft (DFG) in the framework of the

SFB 925 "Light induced dynamics and control of correlated quantum systems".

Appendix A: ML-MCTDHF

The Multi-Layer Multi-Configuration Time-Dependent Hartree method for multicomponent quantum gases (ML-MCTDHF) [10] constitutes a variational numerical ab-initio method for investigating both the stationary properties and in particular the non-equilibrium quantum dynamics of mixture ensembles covering the weak and strong correlation regimes. Its multi-layer feature enables us to deal with multispecies systems (e.g. Bose-Bose, Fermi-Fermi or Bose-Fermi mixtures), multidimensional or mixed dimensional systems in an efficient manner. The multiconfigurational expansion of the wavefunction in the ML-MCTDHF method takes into account higher band effects which renders this approach suitable for the investigation of systems governed by temporally varying Hamiltonians, where the system can be excited to higher bands especially during the dynamics. Finally within the ML-MCTDHF approach the representation of the wavefunction is performed by variationally optimal (time-dependent) single particle functions (SPFs) and expansion coefficients $A_{i_1...i_S}(t)$ which makes the truncation of the Hilbert space optimal when employing the optimal time-dependent moving basis. The requirement for convergence demands a sufficient number of SPFs such that the numerical exactness of the method is guaranteed. Therefore, the number of SPFs has to be increased until the quantities of interest acquire the corresponding numerical accuracy.

In a generic mixture system consisting of N_σ atoms (bosons or fermions) of species $\sigma = 1, 2, \dots, S$ the main concept of the ML-MCTDHF method is to solve the time-dependent Schrödinger equation $i\partial_t|\Psi\rangle = \hat{H}|\Psi\rangle$ as an initial value problem, $|\Psi(0)\rangle = |\Psi_0\rangle$, by expanding the total wave-function in terms of Hartree products

$$|\Psi(t)\rangle = \sum_{i_1=1}^{M_1} \sum_{i_2=1}^{M_2} \dots \sum_{i_S=1}^{M_S} A_{i_1...i_S}(t) \times |\psi_{i_1}^{(1)}(t)\rangle \dots |\psi_{i_S}^{(S)}(t)\rangle. \quad (\text{A1})$$

Here each species state $|\psi_i^{(\sigma)}\rangle$ ($i = 1, 2, \dots, M_\sigma$) corresponds to a system of N_σ indistinguishable atoms (bosons or fermions) and describes a many-body state of a subsystem composed of σ -species particles. The expansion of each species state in terms of bosonic or fermionic number states $|\vec{n}(t)\rangle^\sigma$ reads

$$|\psi_i^{(\sigma)}\rangle = \sum_{\vec{n}||\sigma} C_{i;\vec{n}}^\sigma(t) |\vec{n}(t)\rangle^\sigma, \quad (\text{A2})$$

where each σ atom can occupy m_σ time-dependent SPFs $|\varphi_j^{(\sigma)}\rangle$. The vector $|\vec{n}\rangle = |n_1, n_2, \dots, n_{m_\sigma}\rangle$ contains the

occupation number n_j of the j -th SPF that obeys the constraint $n_1 + n_2 + \dots + n_{m_\sigma} = N_\sigma$. Note that for the bosonic case $n_j = 0, 1, 2, \dots, N$ while for the fermionic case only $n_j = 0, 1$ are permitted due to the Pauli exclusion principle.

In the present work, we focus on the case of a single fermionic species in one spatial dimension where the ML-MCTDHF is equivalent to MCTDHF. To be self-contained, let us briefly discuss the ansatz for the many-body wavefunction and the procedure for the derivation of the equations of motion. The many-body wavefunction which is a linear combination of time-dependent Slater determinants reads

$$|\Psi(t)\rangle = \sum_{\vec{n}} C_{\vec{n}}(t) |n_1, n_2, \dots, n_M; t\rangle. \quad (\text{A3})$$

Here M denotes the total number of SPFs and the summation is performed over all possible combinations which retain the total number of fermions. In the limit in which M approaches the number of grid points the above expansion becomes numerically exact in the sense of a full configuration interaction approach. Another limiting case of the used expansion refers to the case that M equals the number of particles, being referred to in the literature as Time-Dependent Hartree Fock (TDHF). The Slater determinants in (A3) can be expanded in terms of the creation operators $a_j^\dagger(t)$ for the j -th orbital $\varphi_j(t)$ as follows

$$|n_1, n_2, \dots, n_M; t\rangle = \frac{1}{\sqrt{n_1! n_2! \dots n_M!}} (a_1^\dagger)^{n_1} (a_2^\dagger)^{n_2} \dots (a_M^\dagger)^{n_M} |vac\rangle, \quad (\text{A4})$$

satisfying the standard fermionic anticommutation relations $[a_i(t), a_j^\dagger(t)]_- = \delta_{ij}$, etc. To determine the time-dependent wave function $|\Psi\rangle$, we have to find the equations of motion for the coefficients $C_{\vec{n}}(t)$ and the orbitals (which are both time-dependent). To derive the equations of motion for the mixture system one can employ various approaches such as the Lagrangian, McLachlan or the Dirac-Frenkel variational principle, each of them leading to the same result. Following the Dirac-Frenkel variational principle

$$\langle \delta\Psi | i\partial_t - \hat{H} | \Psi \rangle = 0, \quad (\text{A5})$$

we can determine the time evolution of all the coefficients $C_{\vec{n}}(t)$ in the ansatz (A3) and the time dependence of the orbitals $|\varphi_j\rangle$. In this manner, we end up with a set of M non-linear integro-differential equations of motion for the orbitals $\varphi_j(t)$, which are coupled to the $\frac{M!}{N!(M-N)!}$ linear equations of motion for the coefficients $C_{\vec{n}}(t)$. These equations are the well-known MCTDHF equations of motion [17, 18].

Within our implementation, a discrete variable representation (DVR) scheme is applied, and in particular we adopt the sin-DVR, which intrinsically implements hard-wall boundaries conditions. Furthermore, for the cases

of three and five fermions, six and ten SPFs have been used, respectively, i.e. the number of SPFs being twice the number of the particles. As it turned out, the number of major occupied natural orbitals for both cases, reflecting the convergence of the simulation with respect to the number of SPFs, is equal to the number of particles. This indicates that one just needs to use as many SPFs as there are fermions in order to reach a converged simulation. Finally, in the simulation of the eleven-fermion case, only eleven SPFs have been used.

Appendix B: Semiclassical equations

We firstly re write the Hamiltonian of equation (1) in the Hubbard form. Upon the lowest-band Wannier states $\{|L\rangle_i, |R\rangle_i\}_{i=1}^N$, we define a set of basis vectors of $\{|S\rangle_i, |A\rangle_i\}_{i=1}^N$, where $|S(A)\rangle_i \equiv (|L\rangle_i + (-)|R\rangle_i)/\sqrt{2}$ denote the corresponding symmetric (anti-symmetric) superposition within the i -th supercell. By regarding $|S\rangle_i/|A\rangle_i$ as a pseudo-spin state of $|\downarrow\rangle/|\uparrow\rangle$, we introduce the Pauli matrices σ_α , with $\alpha = x, y, z$ for these basis vectors. We focus on the evolution of the system after the tilt is removed, and the corresponding Hamiltonian can then be expressed in this basis as

$$\begin{aligned} \hat{H} = & J \sum_{i=1}^N \sigma_z(i) + \sum_{i=1}^{N-1} V(S_i^+ S_{i-1}^- + h.c.) \\ & + \sum_{i=1}^{N-1} V(S_i^+ S_{i-1}^+ + H.c.) + U(\sigma_x(1) - \sigma_x(N)), \end{aligned} \quad (\text{B1})$$

where J refers to the intra-cell hopping strength, and V , U are determined by the interaction strength. In this reduced Hamiltonian, we approximate the dipolar interaction by a nearest-neighbor interaction and neglect the inter-cell hopping, which is valid within the weak interaction regime considered in this work [50].

Based on equation (B1), $|\Psi(t)\rangle$ can be solved analytically by perturbation theory. It turns out to be enough to use the first order perturbation. In the perturbation treatment, we take the last two terms in equation (B1) as a perturbation. To zero-th order, the ground state is given by equation (2). The first-order correction of degenerate perturbation theory gives that a set of low-lying excited states bunch into a band on top of the ground state, and the eigenstates in this first excited band can be expressed as

$$|k\rangle = \sum_{i=1}^N \sin\left(\frac{k i \pi}{N+1}\right) |i\rangle_-, \quad (\text{B2})$$

where $|i\rangle_- = (\prod_{n \in [1, i-1] \cup [i+1, N]} |S\rangle_n) \times |A\rangle_i$. It can be shown that for the collective dynamics considered here, it is enough to focus on the ground state and first excited band. Without loss of generality, we can assume the wave function at time τ , i.e. when V_{pt} vanishes, as $|\Psi(\tau)\rangle =$

$(\alpha|S\rangle_1 + \beta|A\rangle_1) \times \prod_{i=2}^N |S\rangle_i$ with $|\alpha|^2 + |\beta|^2 = 1$. Then $|\Psi(t - \tau)\rangle$ becomes

$$\begin{aligned} |\Psi(t - \tau)\rangle &= e^{-i\epsilon_0(t-\tau)} |G\rangle \langle G | \Psi(\tau)\rangle \\ &+ \sum_{k=1}^N e^{-i\epsilon_k(t-\tau)} |k\rangle \langle k | \Psi(\tau)\rangle \\ &= \alpha e^{-i\epsilon_0(t-\tau)} |G\rangle \\ &+ \sum_{k=1}^N \beta \sin\left(\frac{k\pi}{N+1}\right) e^{-i\epsilon_k(t-\tau)} |k\rangle. \end{aligned} \quad (\text{B3})$$

In the basis of $\{|S\rangle_i, |A\rangle_i\}_{i=1}^N$, $\delta\hat{\rho}_i$ becomes $\sigma_x(i)$. Sub-

stituting this expression and equation (B1) into equation (4), we obtain

$$[[\delta\hat{\rho}_i, \hat{H}], \hat{H}] = 4J^2\sigma_x(i) - 4JV\sigma_z(i) \times (\sigma_x(i+1) + \sigma_x(i-1)). \quad (\text{B4})$$

Further using equation (B3) for the average $\langle \dots \rangle$, it can be proven that $\langle \sigma_z(i)\sigma_x(i \pm 1) \rangle = \langle \sigma_x(i \pm 1) \rangle$. It is then straightforward to obtain the time derivative equation (5).

-
- [1] P. W. Anderson, Concepts in Solids: Lectures on the Theory of Solids. World Scientific Lecture Notes in Physics. World Scientific Pub Co Inc, (1998).
 - [2] S.H. Simon, The Oxford solid state basics. Oxford: Oxford University Press., 1st ed. edition, (2013).
 - [3] J. Bardeen, Cooperative Phenomena. Springer-Verlag, Berlin, Heidelberg, New York, (1973).
 - [4] S. Lepri, R. Livi, and A. Politi, Thermal conduction in classical low-dimensional lattices, Phys. Rep., **377**, 1 (2003).
 - [5] N. Li, J. Ren, L. Wang, G. Zhang, P. Hänggi, and B. Li, Colloquium : Phononics: Manipulating heat flow with electronic analogs and beyond, Rev. Mod. Phys., **84**, 1045 (2012).
 - [6] D. Porras, and J. I. Cirac, Bose-Einstein condensation and strong-correlation behavior of phonons in ion traps., Phys. Rev. Lett. **93**, 263602 (2004).
 - [7] U. Bissbort, D. Cocks, A. Negretti, Z. Idziaszek, T. Calarco, F. Schmidt-Kaler, W. Hofstetter, and R. Gerritsma, Emulating solid-state physics with a hybrid system of ultracold ions and atoms, Phys. Rev. Lett., **111**, 080501 (2013).
 - [8] G. Pupillo, A. Griessner, A. Micheli, M. Ortner, D.-W. Wang, and P. Zoller, Cold atoms and molecules in self-assembled dipolar lattices, Phys. Rev. Lett., **100**, 050402 (2008).
 - [9] M. Ortner, A. Micheli, G. Pupillo, and P. Zoller, Quantum simulations of extended hubbard models with dipolar crystals, New J. Phys., **11**, 055045 (2009).
 - [10] L. Cao, V. Bolsinger, S.I. Mistakidis, G. Koutentakis, S. Krönke, J.M. Schurer and P. Schmelcher, An all-in-all ab-initio approach to multi-component quantum gases of fermions and bosons, **in preparation**.
 - [11] H.-D. Meyer, U. Manthe, and L.S. Cederbaum, The multi-configurational time-dependent hartree approach, Chem. Phys. Lett., **165**, 73 (1990).
 - [12] M. H. Beck, A. Jäckle, G. A. Worth, and H. D. Meyer, The multiconfiguration time-dependent hartree (mctdh) method: a highly efficient algorithm for propagating wavepackets, Phys. Rep., **324**, 1 (2000).
 - [13] H. Wang and M. Thoss, Multilayer formulation of the multiconfiguration time-dependent hartree theory, J. Chem. Phys., **119**, 1289 (2003).
 - [14] U. Manthe, A multilayer multiconfigurational time-dependent hartree approach for quantum dynamics on general potential energy surfaces, J. Chem. Phys., **128**, 164116 (2008).
 - [15] S. Krönke, L. Cao, O. Vendrell, and P. Schmelcher, Non-equilibrium quantum dynamics of ultra-cold atomic mixtures: the multi-layer multi-configuration time-dependent hartree method for bosons, New J. Phys., **15**, 063018 (2013).
 - [16] L. Cao, S. Krönke, O. Vendrell, and P. Schmelcher, The multi-layer multi-configuration time-dependent hartree method for bosons: Theory, implementation, and applications, J. Chem. Phys., **139**, 134103 (2013).
 - [17] O. E. Alon, A. I. Streltsov, and L. S. Cederbaum, Multiconfigurational time-dependent hartree method for bosons: Many-body dynamics of bosonic systems, Phys. Rev. A, **77**, 033613 (2008).
 - [18] O. E. Alon, A. I. Streltsov, K. Sakmann, A. U. J. Lode, J. Grond, and L. S. Cederbaum, Recursive formulation of the multiconfigurational time-dependent hartree method for fermions, bosons and mixtures thereof in terms of one-body density operators, Chem. Phys., **401**, 2 (2012).
 - [19] E. Fasshauer and A. U. J. Axel, Multiconfigurational time-dependent Hartree method for fermions: Implementation, exactness, and few-fermion tunneling to open space, Phys. Rev. A, **93**, 033635 (2015).
 - [20] A. I. Streltsov, O. E. Alon, and L. S. Cederbaum, Swift loss of coherence of soliton trains in attractive bose-einstein condensates, Phys. Rev. Lett., **106**, 240401 (2011).
 - [21] S. Krönke and P. Schmelcher, Many-body processes in black and gray matter-wave solitons, Phys. Rev. A, **91**, 053614 (2015).
 - [22] O. E. Alon, A. I. Streltsov, and L. S. Cederbaum, Zoo of quantum phases and excitations of cold bosonic atoms in optical lattices, Phys. Rev. Lett., **95**, 030405 (2005).
 - [23] S. Zöllner, H.-D. Meyer, and P. Schmelcher, Few-boson dynamics in double wells: From single-atom to correlated pair tunneling, Phys. Rev. Lett., **100**, 040401 (2008).
 - [24] K. Sakmann, A. I. Streltsov, O. E. Alon, and L. S. Cederbaum, Exact quantum dynamics of a bosonic josephson junction, Phys. Rev. Lett., **103**, 220601 (2009).
 - [25] L. Cao, I. Brouzos, S. Zöllner, and P. Schmelcher, Interaction-driven interband tunneling of bosons in the triple well, New J. Phys., **13**, 033032 (2011).
 - [26] S. I. Mistakidis, L. Cao, and P. Schmelcher, Interaction quench induced multimode dynamics of finite atomic en-

- sembles, *J. Phys. B: At. Mol. Opt. Phys.* **47**, 225303 (2014).
- [27] S. I. Mistakidis, L. Cao, and P. Schmelcher, Negative-quench-induced excitation dynamics for ultracold bosons in one-dimensional lattices, *Phys. Rev. A* **91**, 033611 (2014).
- [28] S. I. Mistakidis, T. Wulf, A. Negretti, and P. Schmelcher, Resonant quantum dynamics of few ultracold bosons in periodically driven finite lattices, *J. Phys. B: At. Mol. Opt. Phys.* **48**, 244004 (2015).
- [29] T. Lahaye, C. Menotti, L. Santos, M. Lewenstein, and T. Pfau, The physics of dipolar bosonic quantum gases. *Rep. Prog. Phys.*, **72** 126401, (2009).
- [30] M. A. Baranov, M. Dalmonte, G. Pupillo, and P. Zoller, Condensed matter theory of dipolar quantum gases, *Chem. Rev.*, **112** 5012, 2012.
- [31] S. Yi, T. Li, and C. P. Sun, Novel quantum phases of dipolar bose gases in optical lattices, *Phys. Rev. Lett.*, **98** 260405, (2007).
- [32] B. Capogrosso-Sansone, C. Trefzger, M. Lewenstein, P. Zoller, and G. Pupillo, Quantum phases of cold polar molecules in 2d optical lattices, *Phys. Rev. Lett.*, **104** 125301, (2010).
- [33] P. Hauke, F. M. Cucchietti, A. Müller-Hermes, M.-C. Banuls, J. I. Cirac, and M. Lewenstein, Complete devils staircase and crystal-superfluid transitions in a dipolar xxz spin chain: a trapped ion quantum simulation, *New J. Phys.*, **12** 113037, (2010).
- [34] H. Kadau, M. Schmitt, M. Wenzel, C. Wink, T. Maier, I. Ferrier-Barbut, and T. Pfau, Observing the rosenzweig instability of a quantum ferrofluid. *Nature*, **530**, 7589 (2016).
- [35] I. Ferrier-Barbut, H. Kadau, M. Schmitt, M. Wenzel, and T. Pfau, Observation of quantum droplets in a strongly dipolar bose gas, *Phys. Rev. Lett.*, **116**, 215301 (2016).
- [36] A. Micheli, G. K. Brennen, and P. Zoller, A toolbox for lattice-spin models with polar molecules, *Nat. Phys.*, **2**, 341 (2006).
- [37] A. V. Gorshkov, S. R. Manmana, G. Chen, J. Ye, E. Demler, M. D. Lukin, and A. M. Rey, Tunable superfluidity and quantum magnetism with ultracold polar molecules, *Phys. Rev. Lett.*, **107**, 115301 (2011).
- [38] R. A. H. Kaden, S. R. Manmana, M. Foss-Feig, and A. M. Rey, Far-from-equilibrium quantum magnetism with ultracold polar molecules, *Phys. Rev. Lett.*, **110**, 075301 (2013).
- [39] X. Zhou, X. Xu, X. Chen, and J. Chen, Magic wavelengths for terahertz clock transitions, *Phys. Rev. A*, **81**, 012115 (2010).
- [40] B. Olmos, D. Yu, Y. Singh, F. Schreck, K. Bongs, and I. Lesanovsky, Long-range interacting many-body systems with alkaline-earth-metal atoms, *Phys. Rev. Lett.*, **110**, 143602 (2013).
- [41] S. Baier, M. J. Mark, D. Petter, K. Aikawa, L. Chomaz, Z. Cai, M. Baranov, P. Zoller, and F. Ferlaino, Extended bose-hubbard models with ultracold magnetic atoms. *Science*, **352**, 6282 (2016).
- [42] K.-K. Ni, S. Ospelkaus, M. H. G. de Miranda, A. Pe'er, B. Neyenhuis, J. J. Zirbel, S. Kotochigova, P. S. Julienne, D. S. Jin, and J. Ye, A high phase-space-density gas of polar molecules, *Science*, **322**, 5899 (2008).
- [43] J. Deiglmayr, A. Grochola, M. Repp, K. Mörtlbauer, C. Glück, J. Lange, O. Dulieu, R. Wester, and M. Weidemüller, Formation of ultracold polar molecules in the rovibrational ground state, *Phys. Rev. Lett.*, **101**, 133004 (2008).
- [44] B. Yan, S. A. Moses, B. Gadway, J. P. Covey, K. R. A. Hazzard, A. M. Rey, D. S. Jin, and J. Ye, Observation of dipolar spin-exchange interactions with lattice-confined polar molecules, *Nature*, **501**, 7468 (2013).
- [45] M. Guo, B. Zhu, B. Lu, X. Ye, F. Wang, R. Vexiau, N. Bouloufa-Maafa, G. Quemener, O. Dulieu, and D. Wang, Creation of an ultracold gas of ground-state dipolar ^{23}Na ^{87}Rb molecules, *Phys. Rev. Lett.*, **116**, 205303 (2016).
- [46] A. Frisch, M. Mark, K. Aikawa, S. Baier, R. Grimm, A. Petrov, S. Kotochigova, G. Quemener, M. Lepers, O. Dulieu, and F. Ferlaino, Ultracold dipolar molecules composed of strongly magnetic atoms, *Phys. Rev. Lett.*, **115**, 203201 (2015).
- [47] S. Fölling, S. Trotzky, P. Cheinet, M. Feld, R. Saers, A. Widera, T. Müller, and I. Bloch, Direct observation of second-order atom tunnelling, *Nature*, **448**, 1029 (2007).
- [48] H.-N. Dai, B. Yang, A. Reingruber, X.-F. Xu, X. Jiang, Yu-Ao Chen, Z.-S. Yuan, and J.-W. Pan, Generation and detection of atomic spin entanglement in optical lattices, *Nature Phys.*, **3705** (2016).
- [49] M. Lohse, C. Schweizer, O. Zilberberg, M. Aidelsburger, and I. Bloch, A thouless quantum pump with ultracold bosonic atoms in an optical superlattice, *Nature Phys.*, **12**, 350 (2016).
- [50] X. Yin, L. Cao, and P. Schmelcher, Magnetic kink states emulated with dipolar superlattice gases, *EPL*, **110**, 26004 (2015).
- [51] L. Cao, I. Brouzos, B. Chatterjee, and P. Schmelcher, The impact of spatial correlation on the tunneling dynamics of few-boson mixtures in a combined triple well and harmonic trap, *New J. Phys.*, **14**, 093011 (2012).
- [52] S. Will, T. Best, U. Schneider, L. Hackermüller, D.-S. Luhmann, and I. Bloch, Time-resolved observation of coherent multi-body interactions in quantum phase revivals, *Nature*, **465** 7295 (2010).